

Full Articles

Carbon and silicon triangulenes: searching for molecular magnets

O. A. Gapurenko,^a A. G. Starikov,^b R. M. Minyaev,^{a*} and V. I. Minkin^a

^a*Institute of Physical and Organic Chemistry at Southern Federal University,
194/2 prosp. Stachki, 344090 Rostov-on-Don, Russian Federation.*

Fax: +7 (863) 243 4667. E-mail: minyaev@ipoc.rsu.ru

^b*Southern Scientific Center, Russian Academy of Sciences,
41 ul. Chekhova, 344006 Rostov-on-Don, Russian Federation*

The structures of a number of neutral high-spin, triangular carbon and silicon systems were studied and their stabilities were predicted using the density functional theory methods (B3LYP functional with the 6-311++G** and 6-311+G** basis sets). The calculated spin-spin coupling constants have high positive values, thus indicating strong ferromagnetic interactions in the title systems.

Key words: triangulenes, alternant non-Kekulé structures, high-spin molecules, molecular magnets, molecular modeling, quantum chemical calculations, density functional theory, B3LYP/6-311+G** and B3LYP/6-311++G** methods.

Design of nonmetallic magnetic materials based on carbon and other non-metals is not only a technologically important task, but also offers prospects for integration of spin and molecular electronics. At present, the state of the art in chemistry and technology of graphite and graphene is such that one can synthesize small graphene species which can exhibit magnetic properties.

Alternant hydrocarbons with different number of atoms of the types *a* and *b* (type-*a* atoms alternate with type-*b* atoms) are characterized by high ground-state multiplicity; the total spin of the system is given by

$$S = \frac{|n(a) - n(b)|}{2}, \quad (1)$$

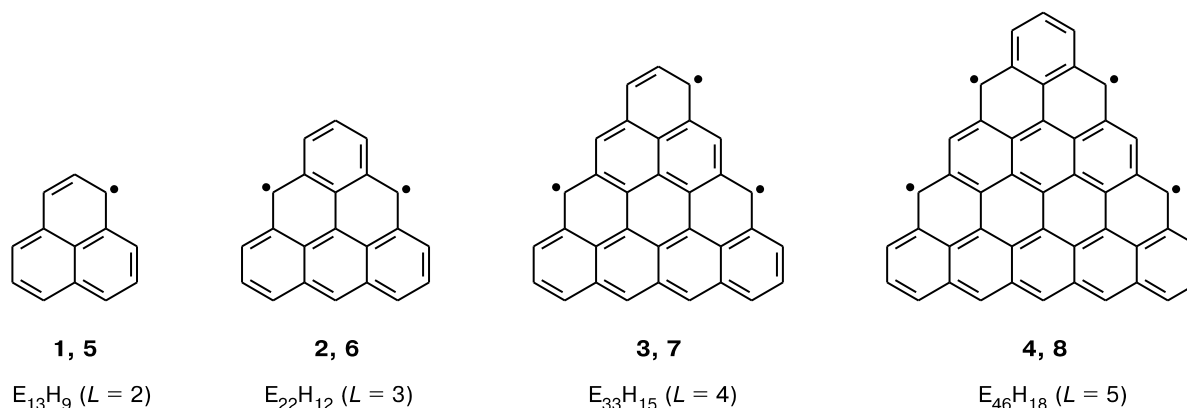
where *S* is the spin of the system, *n(a)* is the number of the type-*a* atoms, and *n(b)* is number of the type-*b* atoms.^{1,2}

These hydrocarbons can be of interest for the design of carbon magnetic materials.

Alternant hydrocarbons include triangular graphene molecules **1**–**4** with zigzag edges (triangulenes) derived from phenalenyl radical **1** as the parent structure. A feature of triangulenes is an increase in the ground-state multiplicity with an increase in the size of the molecule. The total spin of a triangulene molecule can be calculated using a simplified relation

$$S = (L - 1)/2, \quad (2)$$

where *L* is the number of "rows" (or rings on one side of the "triangle").^{1,2} Then the ground-state multiplicity (*M*) of a triangulene is given by *M* = *L*. Triangulenes also belong to hydrocarbons that cannot be represented by Kekulé structures.



E = C (1–4), Si (5–8)

Phenalenyl radical **1** was studied experimentally in the forms of a symmetric tri-*tert*-butyl derivative³ and oxophenalenoxyls.^{4,5} According to X-ray study³ of 2,5,8-tri-*tert*-butylphenalenyl radical, in the crystalline state the phenalenyl fragment has a slightly distorted symmetry D_{3h} . The apex carbon atoms bonded to *tert*-butyl groups deviate by 0.064–0.070 Å from the least-squares plane of the ring. The carbon–carbon bond lengths in the phenalenyl fragment range from 1.374 to 1.421 Å (see Ref. 3), which is comparable with the bond lengths in naphthalene molecule. An analysis of the spin density distribution, EPR spectra, and nucleus-independent chemical shifts (NICS)⁶ of isomeric oxophenalenoxyls allowed one to establish that the unpaired electron is localized on the antiaromatic ring of the system.⁵

The next, after phenalenyl radical, representative of the family is triangulene **2** (or Clar hydrocarbon) known since 1941.⁷ It was synthesized⁸ by Clar as diquinone in 1953 but appeared to be unstable, namely, it immediately polymerized or rearranged. Symmetric derivatives (triplet biradicals) were obtained more recently. 2,6,10-Tri-*tert*-butyltriangulene is kinetically unstable, *viz.*, it undergoes oligomerization in solution,⁹ while trioxytriangulene is stable *in vacuo* at ~20 °C, being, however, very sensitive to atmospheric oxygen.¹⁰

A change (decrease) in the initial symmetry of triangulene derivatives leads to a change in the spin state of the system. For instance, dioxytriangulene has a singlet ground state¹¹ in contrast to trioxytriangulene¹⁰: two substituents significantly change the energy levels of the initial HOMOs occupied by the unpaired electrons; this allows them to form a pair and leads to a change in the ground spin state.¹¹ Probably, Clar's diquinonetriangulene appeared to unstable for the same reason.

Earlier, it was shown theoretically that the energy of the triplet state of triangulene **2** is 20 kcal mol^{−1} lower than that of its singlet state.¹² Recent plane-wave DFT calculations¹³ showed that triangulenes have high-spin ground states up to $L = 15$.

In the present study, we report the results of B3LYP/6-311++G** and B3LYP/6-311+G** DFT quantum chemical calculations of triangular graphene molecules with zigzag edges ($L = 2–5$) and their silicon analogs.

Calculation Procedure

Calculations were carried out using the Gaussian-03 program.¹⁴ All stationary points on the potential energy surface (PES) were identified by calculating the Hesse matrix (λ). For each structure, we calculated all possible spin states and showed the energy preferableness (from 5 to 37 kcal mol^{−1}) for the system to exist in the spin state with the maximum possible spin value (Tables 1 and 2).

We failed to locate symmetric structures of low-spin states, mainly C_1 systems were localized. Moreover, the wave functions of four low-spin systems including **2a** and **6a** ($L = 3$, Table 1) as

Table 1. Results of B3LYP/6-311++G** calculations^a of structures 1–4

Structure	Symmetry	Formula	M	ΔE	ΔE_{ZPE}	λ	ω_1
1	D_{3h}	$C_{13}H_9$	2	—	—	0	160.5
2	D_{3h}	$C_{22}H_{12}$	3	0	0	0	91.1
2a ^b	C_1	$C_{22}H_{12}$	1	7.7	8.7	0	89.1
3	C_s	$C_{33}H_{15}$	4	0	0	0	60.1
3a	C_1	$C_{33}H_{15}$	2	7.9	7.3	0	58.6
4	C_1	$C_{46}H_{18}$	5	0	0	0	40.4
4a	C_1	$C_{46}H_{18}$	3	9.0	7.4	0	41.7
4b ^c	C_s	$C_{46}H_{18}$	1	36.5	37.6	0	39.8

^a Here and in Table 2, M is the multiplicity of the system; $\Delta E/\text{kcal mol}^{-1}$ is the relative energy of the isomer; $\Delta E_{\text{ZPE}}/\text{kcal mol}^{-1}$ is the relative energy of the isomer calculated with inclusion of zero-point vibrational energy (ZPE); λ is the number of negative eigenvalues of the Hessian; and ω_1/cm^{-1} is the minimum harmonic vibrational frequency.

^b The wave function has internal instability.

^c The wave function is unstable on going from RHF to UHF.

Table 2. Results of B3LYP/6-311++G** calculations of structures 5–9

Structure	Symmetry	Formula	<i>M</i>	ΔE	ΔE_{ZPE}	λ	ω_1
5	C_{3v}	Si ₁₃ H ₉	2	—	—	0	46.1
6	C_{3v}	Si ₂₂ H ₁₂	3	0	0	0	30.0
6a *	C_s	Si ₂₂ H ₁₂	1	11.2	11.3	0	23.8
7	C_{3v}	Si ₃₃ H ₁₅	4	0	0	0	16.6
7a	C_1	Si ₃₃ H ₁₅	2	5.3	5.1	0	15.6
8	C_{3v}	Si ₄₆ H ₁₈	5	0	0	0	11.4
8a	C_1	Si ₄₆ H ₁₈	3	6.0	5.3	1	<i>i</i> 238.3
8b *	C_1	Si ₄₆ H ₁₈	1	21.3	21.1	0	9.7
9	D_{3d}	Si ₆ H ₆	1	0	0	0	103.7
9a	D_{6h}	Si ₆ H ₆	1	2.3	2.1	1	<i>i</i> 215.2

* The wave function is unstable on going from RHF to UHF.

well as **4b** and **8b** ($L = 5$, Table 2) show either an internal instability or instability on going from RHF to UHF. One low-spin silicon system (**8a**) was located as transition state rather than a minimum on the PES.

Results and Discussion

Triangulene hydrocarbons. Geometrically, the ground-state carbon systems **1** and **2** ($L = 2, 3$) have a D_{3h} symmetry; however, their electronic properties (Mulliken atomic charges, spin density) and the NICS values correspond to a lower symmetry C_{2v} (see Fig. 1). As the size of the system increases, its planarity violates, namely, the planar D_{3h} structure **3** ($L = 4$) in the high-spin state corresponds to a transition state ($\lambda = 1$), whereas the planar D_{3h} structure **4** ($L = 5$) in the ground state corresponds to a threefold point ($\lambda = 3$) on the PES. In nonplanar structures **3** and **4** of symmetry C_s and C_1 , respectively, the atoms deviate from the initial plane up to 0.003 Å (**3**) and 0.004 Å (**4**).

The apex carbon–carbon bonds in the triangulenes in question appeared to be the shortest (1.390 Å in systems **2–4** and 1.391 Å in radical **1**) and close to carbon–carbon bond lengths in benzene (1.394 Å) calculated by the same method with the same basis set. Carbon–carbon bonds along the triangulene perimeters are longer, *viz.*, 1.419–1.420 Å in systems **2–4** (*cf.* 1.417 Å in phenalenyl **1**). For the middle region of the perimeter calculations predict a constant value of 1.408–1.409 Å. The longest carbon–carbon bonds connect the perimeter and the penultimate row of carbon atoms (bond lengths reach up to 1.438 Å in structures **3** and **4**). In the center of triangulenes, carbon–carbon bond lengths are close to those of graphite and graphene (1.421–1.425 Å). The geometric parameters obtained in our calculations are in good agreement with those calculated earlier.¹³

Geometric parameters and other properties discussed below obey a pattern¹³ which divides the triangulene molecules into three regions, namely, the apex and middle

(interior) regions and the perimeter; each region is characterized by its own features.

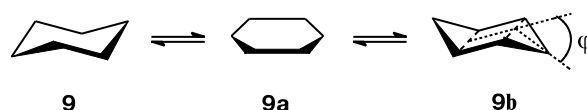
Among the triangulenes under study, radical **1** is characterized by the highest aromaticity; namely, NICS = -2.7 for each ring. For the next members of this family, the general trend is retained, namely, the apex rings with the highest aromaticity (NICS values range from -1.8 for structure **2** to -2.2 for structure **4**) are followed by rings in the middle region (NICS values from -1.4 to -2.0) and peripheral rings with the smallest NICS values (from -0.3 to 0.4 ; positive NICS values mean antiaromatic properties). Unpaired electrons are most probably localized in the peripheral rings.⁵

A clearly seen alternation of the signs of the Mulliken atomic charges on carbons was found only for the perimeters of systems **2–4** except the apex atoms. The signs of the charges on carbon atoms in the middle regions of the large molecules **3** and **4** also alternate; however, the two regions are not connected by alternation.

The spin density distribution shows a strong sign alternation for all triangulene systems, except the phenalenyl radical **1** characterized by almost zero negative spin population on the central carbon atom. Yet another feature characteristic of the spin density distribution in systems **2–4** is that the maximum absolute values of the spin populations are concentrated along the perimeter on type-*a* atoms. Singly occupied orbitals of triangulenes **1–4** are also localized on the type-*a* atoms (see Fig. 2). In systems **3** and **4**, pairs of orbitals (orbitals 107, 108 and 146, 147, respectively) are in fact doubly degenerate (they have almost equal energies).

The energy difference between the HOMO and LUMO decreases as the size of the system increases, being equal to 4.0 (**1**), 3.7 eV (**2**), 3.5 (**3**), and 3.2 eV (**4**). Earlier,¹³ DFT calculations with a plane-wave basis set gave much lower values, namely, 0.53 eV for the phenalenyl radical ($L = 2$) and up to 0.29 eV for the molecule with $L = 15$.

Silicon-hydrogen triangulenes. Replacement of all carbon atoms in compounds **1–4** by silicon atoms leads to new family of high-spin systems. According to our B3LYP/6-311++G** calculations, the ground states of the silicon compounds **5–8** should also have the maximum possible multiplicities defined by expression (2) (see Table 2). Going from carbon triangulenes to the silicon analogs is accompanied by changes in the structural parameters. In contrast to the carbon precursors, the silicon systems **5–8** are non-planar and have a chair-like structure of the silicon cage, similar to that of hexasilabenzene Si₆H₆ for which, according to the results obtained earlier^{15–17} and to our calculations, the planar form **9a** is a transition state between two chair conformers **9** and **9b** (see below; Si atoms are not shown).



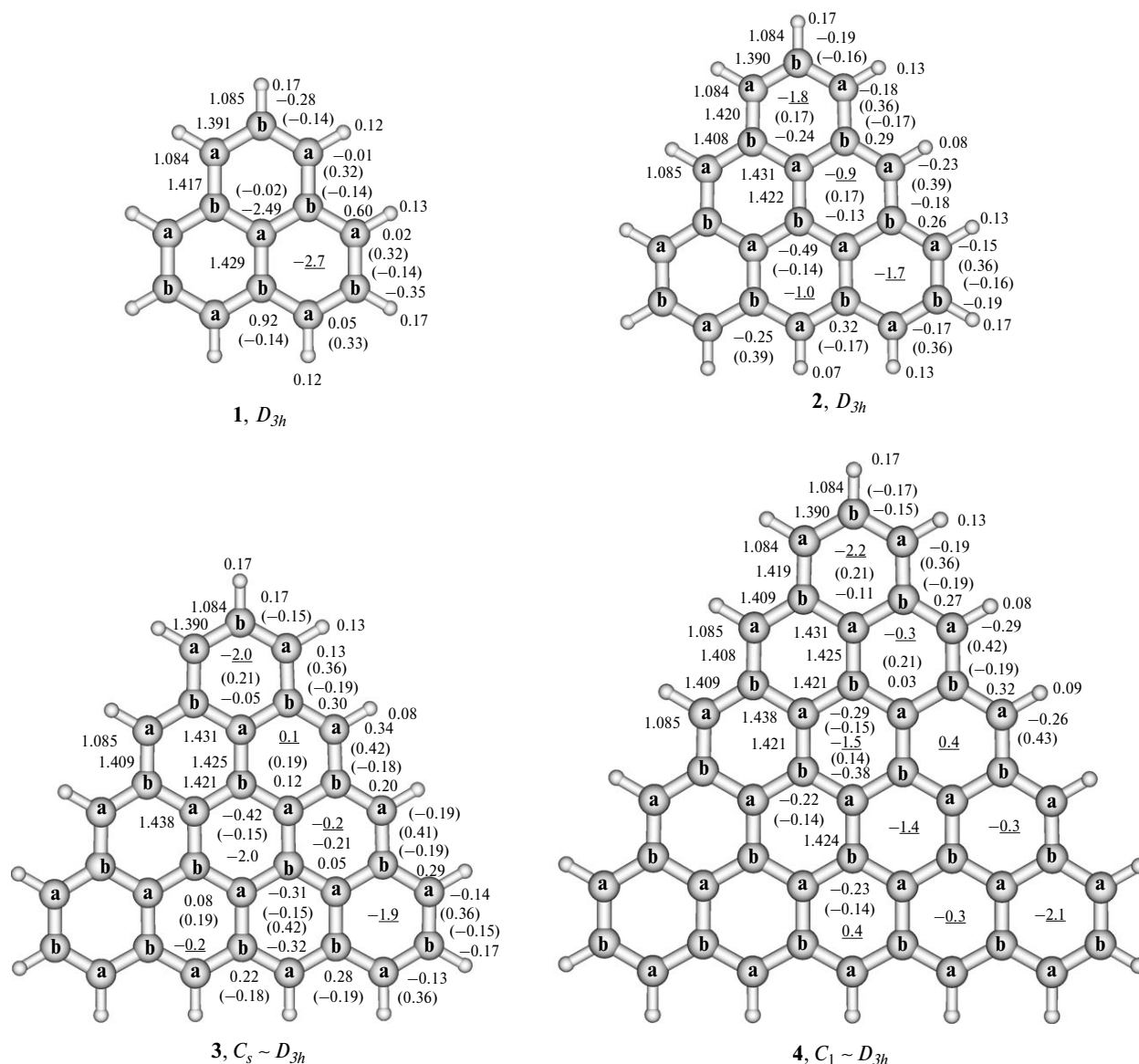


Fig. 1. Bond lengths, Mulliken atomic charges, spin populations on atoms (numbers in parentheses), and NICS values (underlined) in the carbon systems 1–4 calculated by the UB3LYP/6-311++G** method. The Mulliken charge, spin population distributions, and NICS have a lower symmetry C_{2v} . Here and in Figs 2 and 3, the bond lengths are given in Ångströms.

According to our calculations, in structure **9** the deviation φ from the plane is 31.5° , which is more than twice as large as the available¹⁶ values of the angle φ 11.5 – 13.5° (depending on the basis set, HF calculations). According to our calculations for silicon triangulenes **5**–**8**, the angle φ is in the range 30 – 34° .

Trends in the changes of the silicon–silicon bond lengths in the silicon triangulenes **5**–**8** (Fig. 3) and carbon–carbon bonds in the carbon structures 1–4 are analogous, *viz.*, the shortest silicon–silicon bonds (2.242 Å in triangulene **5** and 2.243 Å in systems **6**–**8**) are on the vertices of the silicon molecules and are equal to the silicon–silicon bond lengths in hexasilabenzene **9** (2.242 Å).

Some longer silicon–silicon bonds (2.271 – 2.273 Å), whereas the midpoints of the "triangulenes" are characterized by silicon–silicon bond lengths in the range 2.266 – 2.268 Å. The longest silicon–silicon bonds (to 2.291 Å) connect the outermost and the penultimate set of silicon atoms.

Unlike the carbon systems 1–4, the symmetry of the electronic characteristics of the silicon structures (Mulliken atomic charges, spin density distributions) exactly matches the geometric symmetry (C_{3v}). However, some features appear. For instance, compared with carbon triangulenes, silicon triangulenes show a redistribution of the Mulliken charges over the silicon cage, *viz.*, posi-

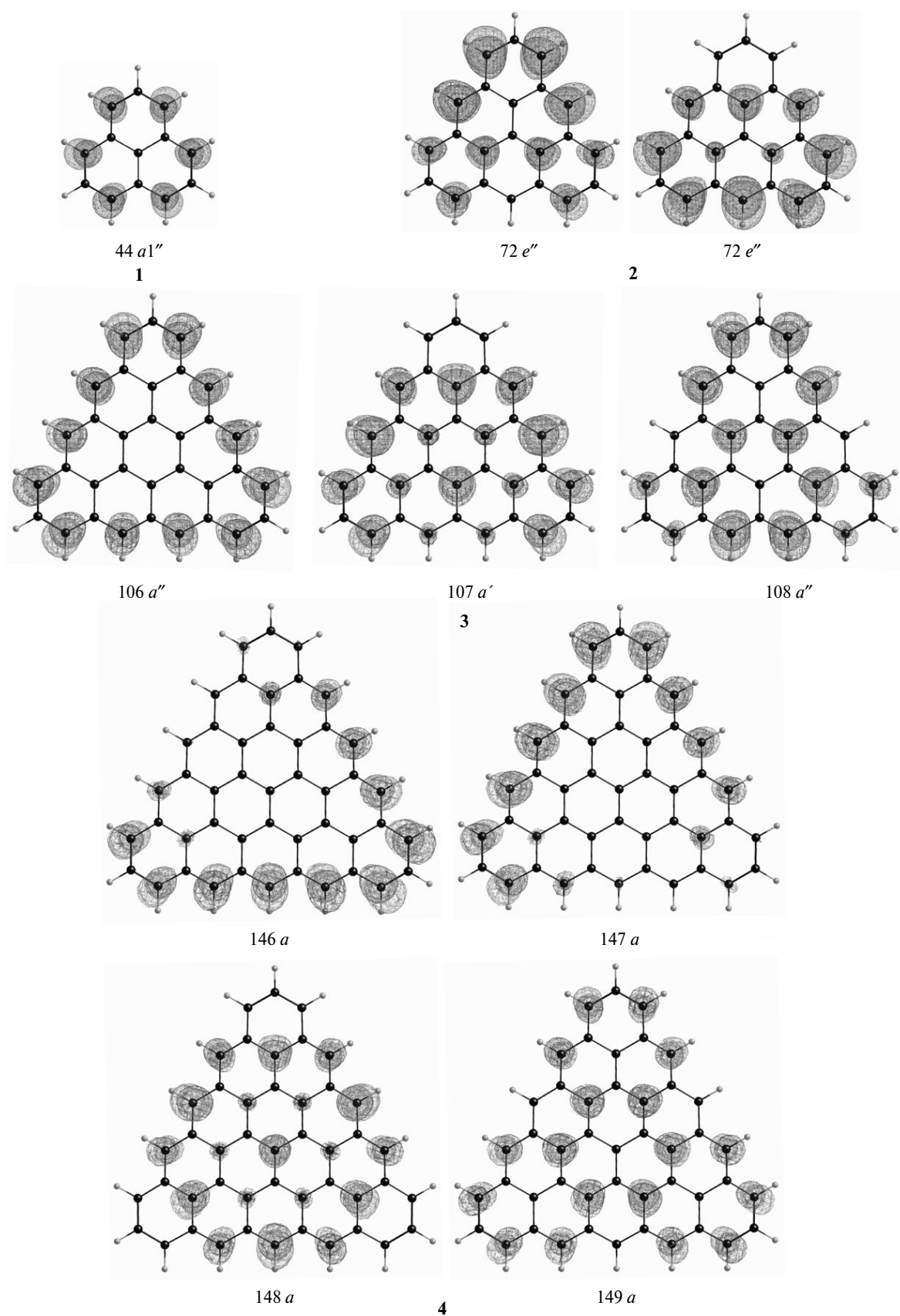


Fig. 2. The highest singly occupied orbitals of carbon systems 1–4.

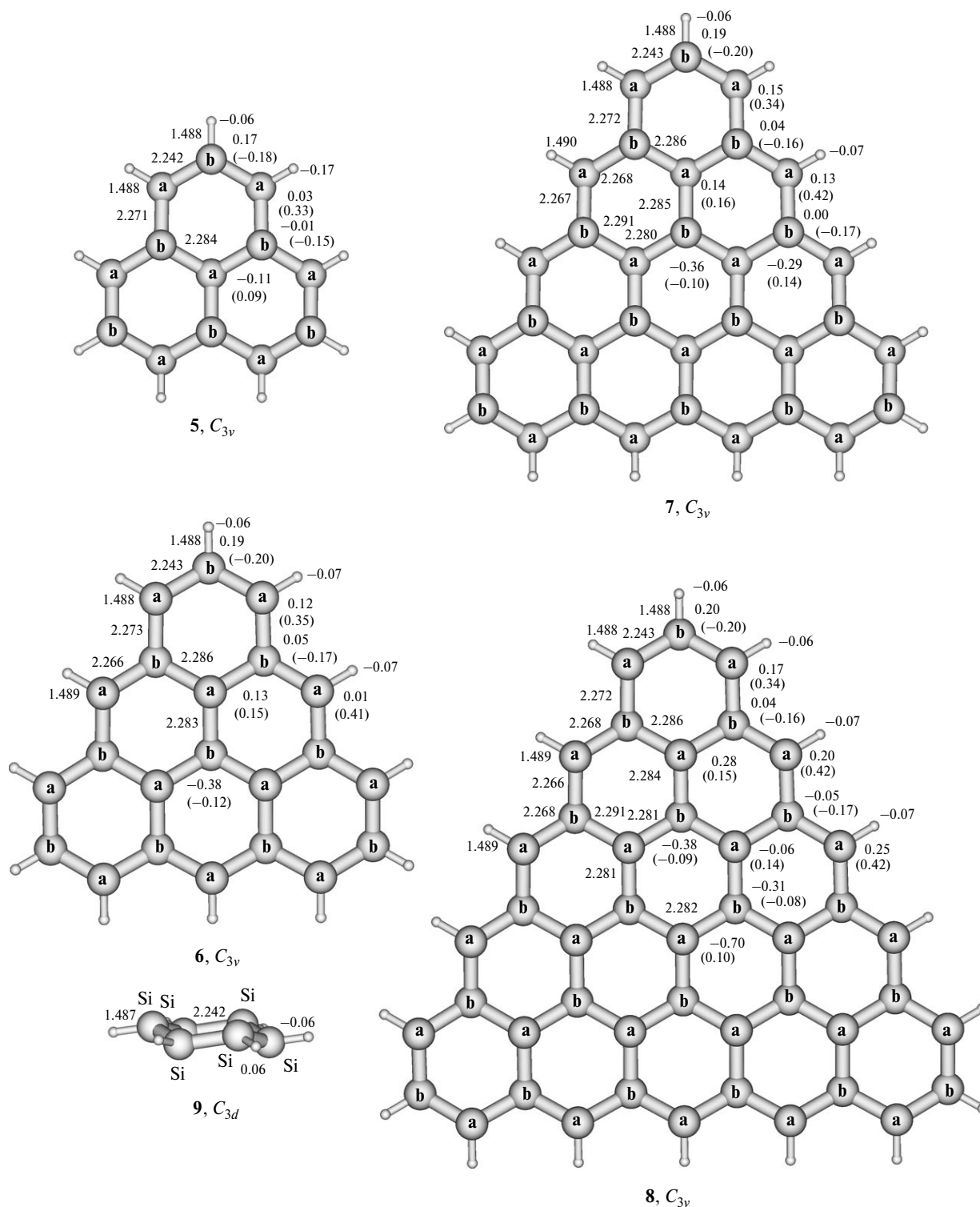


Fig. 3. Bond lengths, Mulliken charges, and spin populations on atoms (numbers in parentheses) of silicon systems 5–9 calculated by the UB3LYP/6-311+G** method.

tive charges are arranged along the perimeter and in the apex regions, while negative charges are concentrated in the middle regions of systems 6–8. The absolute values of negative charges increase toward the cen-

ter and reach a value of -0.70 on the central Si atom of structure 8.

The spin population distributions in the silicon triangelenes 6–8, as in their carbon prototypes 1–4, have

strong alternation and maximum positive values on the type-*a* atoms located along the perimeter. Alternation of the spin density serves an additional confirmation that the state with the maximum possible spin is just the ground state. The spin population distributions along the perimeter of the silicon triangulenes **5**–**8** match those in the carbon systems **2**–**4** both qualitatively and numerically (to an accuracy of 0.02). In the middle regions and on the apex atoms we obtained a larger (to 0.07) scatter of the spin population values compared to the carbon systems.

An analysis of singly occupied higher orbitals of silicon triangulenes revealed that they are almost identical to the corresponding orbitals of carbon triangulenes (see Fig. 2). This, as well as the spin density distribution, indicates a great similarity between the nature of these families. The HOMO–LUMO energy difference of the silicon triangulenes also decreases as the system size increases and is 2.1, 1.9, 1.8, and 1.7 eV for structures **5**, **6**, **7**, and **8**, respectively.

Estimation of spin-spin coupling constants. To estimate prospects of the use of two triangulene families considered as magnetic materials, we calculated the spin-spin coupling constants (magnetic coupling constants, exchange coupling constants) *J* in the second and third (*L* = 3, 4) members of the families of the carbon and silicon compounds. Positive (*J* > 0) values point to ferromagnetic, while negative (*J* < 0) point to antiferromagnetic interaction in the system. We estimated the constants *J* by the broken symmetry method for the systems with unpaired electrons using a scheme proposed elsewhere.¹⁸ For a system with two unpaired electrons on two centers one has

$$J = E_{\text{BS}} - E_{\text{HS}}, \quad (3)$$

where *E*_{BS} is the energy of the broken-symmetry state, *E*_{HS} is the energy of the high-spin ground state (highest symmetry).¹⁸ According to our calculations, *J* = 2450 cm^{−1} for triangulene **2** and *J* = 1673 cm^{−1} for its silicon analog **6**.

For systems with three unpaired electrons occupying the vertices of an equilateral triangle (that can be applied to the triangulene systems studied), we used the relation¹⁸

$$J = (E_{\text{BS}} - E_{\text{HS}})/2. \quad (4)$$

In this case, the calculated *J* value is 2700 cm^{−1} for system **3** and 1857 cm^{−1} for the silicon compound **7**. So large positive *J* values indicate rather strong ferromagnetic interactions in the carbon and silicon triangulenes considered.

Density of spins. The force of a magnet created on the base of new compound will depend on the density of spins. We considered the density of spins in the molecule (ratio of the number of unpaired electrons to the number of C or Si atoms in a given molecule). It is maximum for the compounds with *L* = 3 and 4 (Fig. 4) and then gradually decreases. This suggests that the density of spins in the bulk of the substance will decrease and the magnetic properties

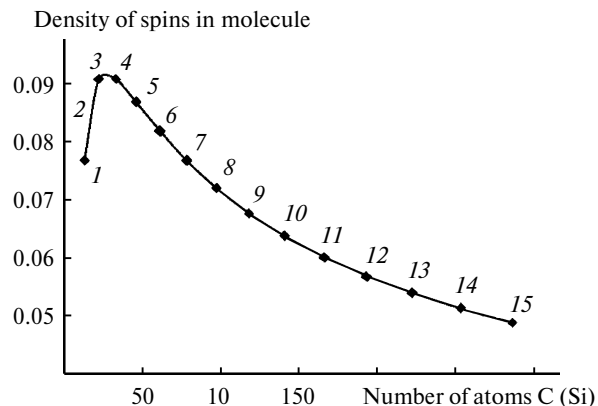


Fig. 4. The densities of spins in molecules calculated as the ratios of the number of unpaired electrons to the number of C or Si atoms in particular molecules. Points 1–15 correspond to the *L* values.

will weaken with increasing the size of the molecule. Taking account of the density of spins will make it possible to create materials with specified magnetic properties.

Thus, our quantum chemical calculations showed that not only hydrocarbon triangulenes, but also their silicon analogs have high ground-state multiplicity which increases with the size of the system. This could serve as a base for engineering of nonmetallic magnetic materials and various sensors based on them.

The study was financially supported by the Russian Foundation for Basic Research (Project No. 10-03-00332), the Council on Grants at the President of the Russian Federation (Program of the State Support of Leading Scientific Schools, Grant NSh-3233.2010.3), and the Ministry of Education and Science of the Russian Federation (Grant RNP.2.2.1.1.2348).

References

1. A. A. Ovchinnikov, *Dokl. Akad. Nauk SSSR*, 1977, **236**, 928 [*Dokl. Phys. Chem. (Engl. Transl.)*, 1977, **236**].
2. A. A. Ovchinnikov, *Theor. Chim. Acta (Berlin)*, 1978, **47**, 297.
3. K. Goto, T. Kubo, K. Yamamoto, K. Nakasuji, K. Sato, D. Shiomi, T. Takui, M. Kubota, T. Kobayashi, K. Yakusi, J. Ouyang, *J. Am. Chem. Soc.*, 1999, **121**, 1619.
4. Y. Morita, T. Ohba, N. Haneda, S. Maki, J. Kawai, K. Hatanaka, K. Sato, D. Shiomi, T. Takui, K. Nakasuji, *J. Am. Chem. Soc.*, 2000, **122**, 4825.
5. Y. Morita, J. Kawai, K. Fukui, S. Nakazawa, K. Sato, D. Shiomi, T. Takui, K. Nakasuji, *Org. Lett.*, 2003, **5**, 3289.
6. P. von R. Schleyer, C. Maerker, A. Dransfeld, H. Jiao, N. J. R. van Eikema Hommes, *J. Am. Chem. Soc.*, 1996, **118**, 6317.
7. E. Clar, in *Aromatische Kohlenwasserstoffe*, Springer-Verlag, Berlin, Germany, 1941, p. 311.
8. E. Clar, D. G. Stewart, *J. Am. Chem. Soc.*, 1953, **75**, 2667.
9. J. Inoue, K. Fukui, T. Kubo, S. Nakazawa, K. Sato, D. Shiomi, Y. Morita, K. Yamamoto, T. Takui, K. Nakasuji, *J. Am. Chem. Soc.*, 2001, **123**, 12702.

10. G. Allinson, R. J. Bushby, J.-L. Paillaud, M. Thornton-Pett, *J. Chem. Soc., Perkin Trans. 1*, 1995, 385.
11. G. Allinson, R. J. Bushby, M. V. Jesudason, J.-L. Paillaud, N. Taylor, *J. Chem. Soc., Perkin Trans. 2*, 1997, 147.
12. M. J. Bearpark, M. A. Robb, F. Bernardi, M. Olivucci, *Chem. Phys. Lett.*, 1994, **217**, 513.
13. M. R. Philpott, F. Cimpoesu, Y. Kawazoe, *Chem. Phys.*, 2008, **354**, 1.
14. M. J. Frisch, G. W. Trucks, H. B. Schlegel, G. E. Scuseria, M. A. Robb, J. R. Cheeseman, J. A. Montgomery, Jr., T. Vreven, K. N. Kudin, J. C. Burant, J. M. Millam, S. S. Iyengar, J. Tomasi, V. Barone, B. Mennucci, M. Cossi, G. Scalmani, N. Rega, G. A. Petersson, H. Nakatsuji, M. Hada, M. Ehara, K. Toyota, R. Fukuda, J. Hasegawa, M. Ishida, T. Nakajima, Y. Honda, O. Kitao, H. Nakai, M. Klene, X. Li, J. E. Knox, H. P. Hratchian, J. B. Cross, C. Adamo, J. Jaramillo, R. Gomperts, R. E. Stratmann, O. Yazyev, A. J. Austin, R. Cammi, C. Pomelli, J. W. Ochterski, P. Y. Ayala, K. Morokuma, G. A. Voth, P. Salvador, J. J. Dannenberg, V. G. Zakrzewski, S. Dapprich, A. D. Daniels, M. C. Strain, O. Farkas, D. K. Malick, A. D. Rabuck, K. Raghavachari, J. B. Foresman, J. V. Ortiz, Q. Cui, A. G. Baboul, S. Clifford, J. Cioslowski, B. B. Stefanov, G. Liu, A. Liashenko, P. Piskorz, I. Komaromi, R. L. Martin, D. J. Fox, T. Keith, M. A. Al-Laham, C. Y. Peng, A. Nanayakkara, M. Challacombe, P. M. W. Gill, B. Johnson, W. Chen, M. W. Wong, C. Gonzalez, J. A. Pople, *Gaussian 03, Revision C.02*, Gaussian Inc., Wallingford, CT, 2004.
15. M. Zhao, B. M. Gimarc, *Inorg. Chem.*, 1996, **35**, 5378.
16. S. Nagase, H. Teramae, T. Kudo, *J. Chem. Phys.*, 1987, **86**, 4513.
17. J. J. Engelberts, R. W. A. Havenith, J. H. van Lenthe, L. W. Jenneskens, P. W. Fowler, *Inorg. Chem.*, 2005, **44**, 5266.
18. E. Ruiz, A. Rodríguez-Fortea, J. Cano, S. Alvarez, P. Alemany, *J. Comput. Chem.*, 2003, **24**, 982.

*Received August 12, 2009;
in revised form March 17, 2011*